

Supplementary Information

Efficient perovskite solar cells fabricated by manganese cations incorporated in hybrid perovskite

Wei Liu,^a Liang Chu,^{a, b} Nanjing Liu,^a Yuhui Ma,^a Ruiyuan Hu,^a Yakui Weng,^b Hui Li,^b Jian
Zhang,^b Xing'ao Li,*^{a, b} Wei Huang*^{a, c}

^a Key Laboratory for Organic Electronics & Information Displays (KLOEID), Synergetic Innovation Center for Organic Electronics and Information Displays (SICOEID), Institute of Advanced Materials (IAM), School of Materials Science and Engineering (SMSE), Nanjing University of Posts and Telecommunications (NUPT), Nanjing 210023, P.R. China

^b New Energy Technology Engineering Laboratory of Jiangsu Province & School of Science, Nanjing University of Posts and Telecommunications (NUPT), Nanjing 210023, China

^c Shaanxi Institute of Flexible Electronics, Northwestern Polytechnical University, Xi'an, 710072, P. R.China

* Corresponding Author:

Email: iamxali@njupt.edu.cn & iamwhuang@njupt.edu.cn

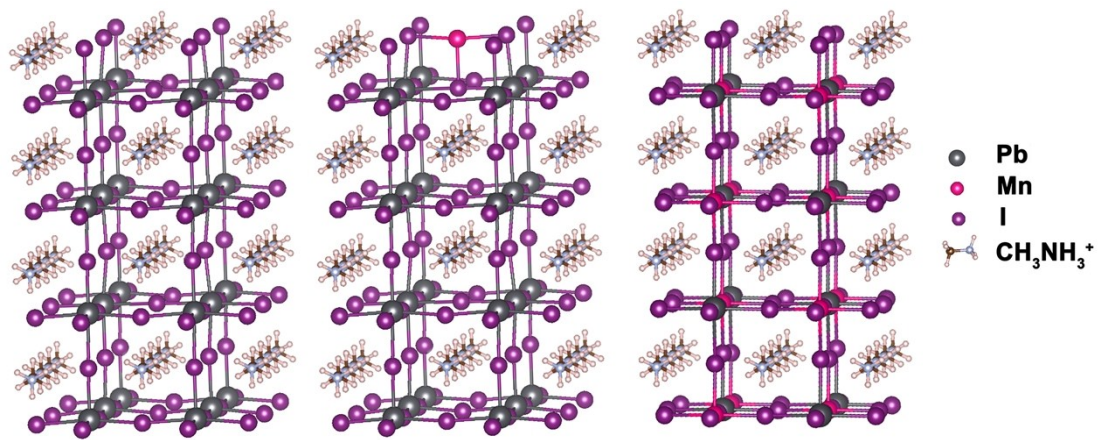


Fig. S1: Schematic diagram for Mn^{2+} can easily insert into the interstices of octahedral $[\text{PbI}_6]^{4-}$ to restrain the generating of vacancy defects.

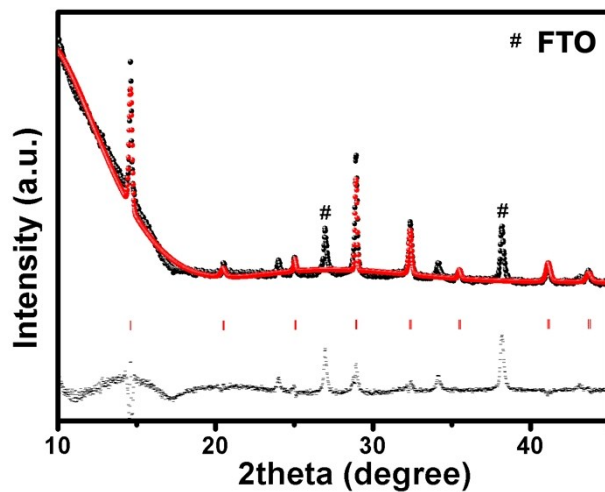


Fig. S2: X-ray diffraction of perovskite/FTO. Black and red line correspond to experimental data and calculation, respectively. Strips (red) indicate positions of the Bragg reflections. Deviation from the fit is shown in dark gray.

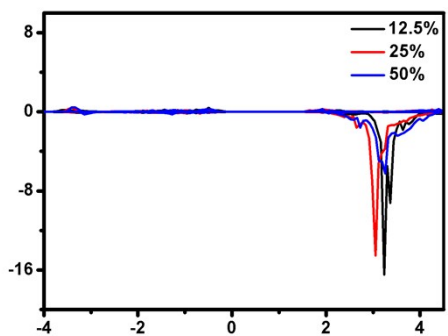


Fig. S3. Computed PDOS for Mn from $\text{MAPb}_{1-x}\text{Mn}_x\text{I}_3$ (where $x = 12.5\%$, 25% , and 50%).

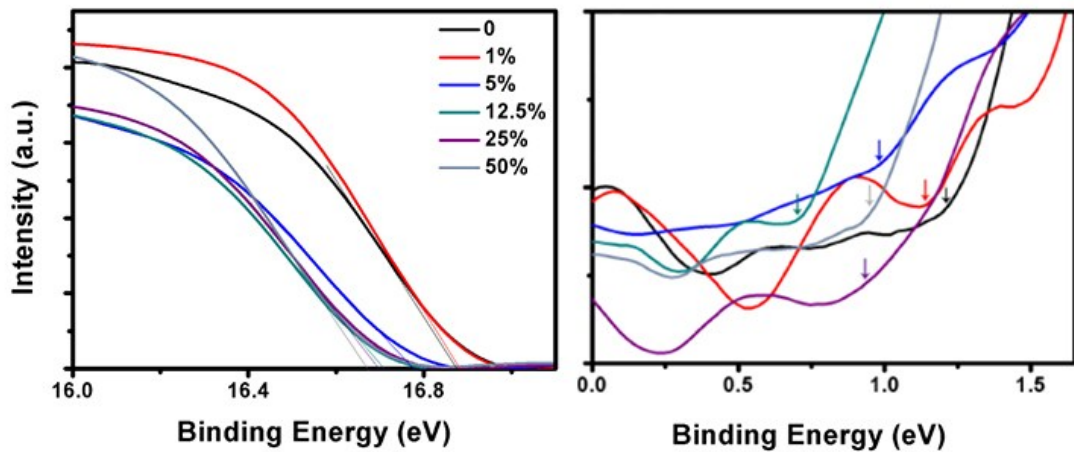


Fig. S4. The detail UPS of $\text{MAPb}_{1-x}\text{Mn}_x\text{I}_3$ (where $x = 0$, 1% , 5% , 12.5% , 25% , and 50%).

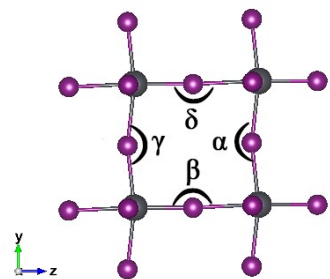


Fig. S5. The octahedral tilting angles of perovskite.

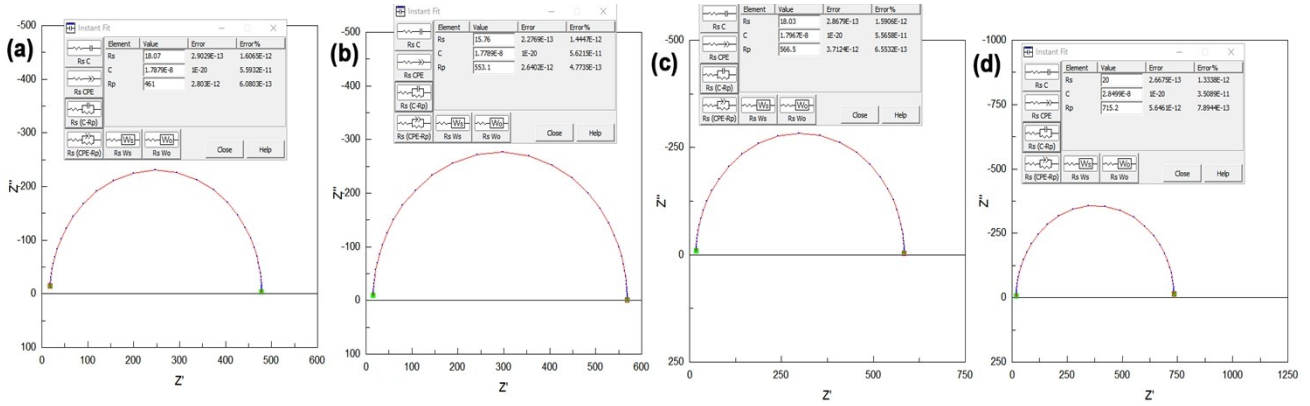


Fig. S6. Data-fitting result of Nyquist plots of PSCs based on (a) excessive 1% Mn-doped MAPbI_3 and $\text{MAPb}_{1-x}\text{Mn}_x\text{I}_3$ (where $x = 0$ (b), 5% (c), and 12.5% (d)). For the data fitting Z-view program (Scribner Associates, Inc.) was used.

Table S1 The octahedral tilting angles and bond length of $\text{MAPb}_{1-x}\text{Mn}_x\text{I}_3$ (where $x = 0$, 12.5%, 25%, and 50%) ($\alpha, \beta, \gamma, \delta$ can be shown in the Fig. S5)

	α	β	γ	δ	Pb-I	Mn-I	Cell volume
0	167.4164	168.5156	167.4164	168.5156	3.06-3.24	-	2144.809697
0.125	166.4376	176.8819	167.6393	177.1387	3.05-3.40	2.76-3.38	2114.037991
0.25	166.7445	176.8288	166.7096	177.0962	3.02-3.38	2.89-3.52	2057.72259
0.5	165.8653	177.0558	165.8841	177.4683	3.07-3.32	2.73-3.65	1898.188338
interstitial	172.5254	177.2448	168.3360	179.0281	3.07-3.40	2.99-3.26	2189.87037

Table S2 The calculated band gap of spin up and spin down.

Mn-incorporated	0	Interstitial	12.5%	25%	50%
up	1.677eV	1.8191eV	1.819eV	1.877eV	1.697eV
down	1.677eV	1.8678eV	1.815eV	1.877eV	1.697eV

Table S3 Fermi energy, valence and conduction band from UPS and calculation.

Mn-doped	high binding energy	Fermi energy (eV)	low binding energy	valence band (eV)	conduction band (eV)	experiment band gap (eV)	calculate band gap (eV)
0	16.95	-4.27	1.22	-5.49	-3.903	1.587	1.677
1%	16.94	-4.28	1.13	-5.41	-3.820	1.590	-
5%	16.78	-4.44	0.99	-5.43	-3.838	1.592	-
12.5%	16.70	-4.52	0.71	-5.23	-3.637	1.593	1.816
25%	16.69	-4.53	0.92	-5.45	-3.850	1.600	1.877
50%	16.66	-4.56	0.93	-5.49	-3.91	1.580	1.697